DIRECT OBSERVATION OF DISLOCATIONS CONSTITUTING SUB-GRAIN BOUNDARIES BY X-RAY TOPOGRAPHY

FUTAGAMI, Koji
Research Institute for Applied Mechanics, Kyushu University : Associate Professor

https://doi.org/10.5109/7173511

出版情報：Reports of Research Institute for Applied Mechanics. 22 (70), pp.231-237, 1975. 九州大学応用力学研究所
バージョン：
権利関係：

Reports of Research Institute for Applied Mechanics
Vol. XXII, No. 70, 1975

DIRECT OBSERVATION OF DISLOCATIONS CONSTITUTING SUB-GRAIN BOUNDARIES BY X-RAY TOPOGRAPHY

By Kōji FUTAGAMI*

Sub-grain boundaries of LiF single crystals with $\sim 10^4$ dislocations/cm^2 are observed by a limited projection topography. In some cases, the parallel dislocation array or the dislocation network constituting a very small tilt or twist boundaries of about 10^{-6} rad., can be separately observed. It is found from determination of the Burgers vectors of dislocations and the analysis of the geometrical configuration of sub-grain boundary that these sub-boundaries are elucidated by the model based on the dislocation theory. A stereo pair of topographs is taken on a square glid dislocation network. A parallel dislocation array along grain boundary in an annealed specimen at high temperature is revealed.

1. Introduction

The direct observation of dislocation configuration constituting a sub-grain boundary plays an important role not only in the interpretation of the dislocation model but also in the verification of dislocation theory. Many works [1] concering this purpose were made.

The etch pit method is limited to the observation of dislocations emerged on the surface only, though this is famous as the observation technique of sub-grain boundary by which the model based on dislocation theory was first proved to be exist in a crystal by comparing the angle between adjacent grains measured by X-ray reflections [2~4]. Many works were made also by the decoration technique [1,5~7] and by the electron microscopy [1]. These techniques, however, introduce damages to the specimen. Moreover, latter requires an extremely thin specimen, so that information obtained is largely different from that obtained in bulk state. It seems that the X-ray diffraction topography, especially the limited projection topography is one of the most useful technique to observe the structure of sub-grain boundaries non-destructively and three-dimensionally.

In previous works [8,9], detailed studies were carried out by the limited projection topography on sub-grain boundaries in LiF single crystals and obtained the conditions for appearance of Pendellösung fringes at sub-boundaries and dislocation images constituting sub-boundaries. This work is a continuation of previous observations. The parallel dislocation array or dislocation networks constituting very small tilt boundary or twist boundary of about 10^{-6} rad., can be sepalately observed. It is found from determination

* Associate Professor, Research Institute for Applied Mechanics, Kyushu University.

of the Burgers vectors and analysis of the geometrical configuration that these sub-boundaries are elucidated by the model based on the dislocation theory. A detailed analysis is made on the sub-boundary where a square grid dislocation network is revealed and a stereo pair of topographs of this is taken to observe three-dimensionally. A parallel dislocation array along a grain boundary in an annealed crystal is also observed.

2. Experimental

LiF single crystals purchased from the Harshaw Chemical Company, which were specified as X-ray analysing grade, were used. A large crystal was cleaved into about one hundred specimens of size 6×5 mm in surface and 2 mm in thickness in such a way that all surfaces of specimens were cube planes. The dislocation density of specimens is about $10^4/cm^2$ in a sub-grain and the size of a sub-grain is about 2 mm^2, therefore, a specimen has a few sub-grains.

Most specimens were used as as-cleaved ones but some specimens were annealed at 600 °C in Ar gas atmosphere for 1 hour with ascending and descending rates of temperature of 5 °C/hr.

The crystal structure of LiF is of the sodium chloride type and its Burgers vector of a complete dislocation $\boldsymbol{b}$ has $a/2\langle110\rangle$ where a is a lattice parameter of LiF($|\boldsymbol{b}|=2.8$ Å for LiF). Therefore, it is favorable to elucidate the structure of sub-grain boundaries based on the dislocation theory. Since absorption coefficient of LiF for X-ray is small compared with other ionic crystals, Si and Ge, relatively thick specimens are used and three-dimensional observations are made.

As observation technique, X-ray diffraction topography of limited projection type was used. Detailed description of this technique has been previously reported by the author [8] and hence further description is omitted. To take the limited projection topography with good resolution, limited portion lying in the crystal of about 0.3 mm thickness containing the exit surface of X-ray was taken by a limiting slit of 100 μm in aperture inserted between the specimen and the plate. The direction of incident X-ray is fixed to the [100] direction in this paper and the projection plane is the inclined to a (100) one by the angle of θ_B which is Bragg angle decided by X-ray and the diffraction plane used. Diffraction vectors $\boldsymbol{g}$ used here are $\boldsymbol{g}=[010]$, [001], [011] and $[0\bar{1}1]$, all of which exist on the (100) plane. (Symmetrical Laue case). Burgers vectors of dislocations constituting sub-boundary can be determined using the invisibility criterion; $\boldsymbol{g}\cdot\boldsymbol{b}=0$.

In order to determine the three-dimensional structure of sub-grain boundaries, a stereo pair of topographs was taken with $\boldsymbol{g}=[010]$ and $[0\bar{1}0]$ and also a series of limited topographs were taken with the change of the position of limiting slit in turn. An image width of an individual grown-in dislocation observed in this experiment is about 8 μm. However, elastic distortion of lattice around one of dislocations forming parallel dislocation array with the same Burgers vector is narrow compared with that of an individual one in a sub-grain as shown by the dislocation theory [10]. As the X-ray contrast is proportional to this elastic distortion, an image width of dislocation constituting sub-boundary becomes narrower than that of grown-in one as calculated in previous paper [8]. Then, the image width of individual dislocation in sub-boudary which is observed actually is about 2 μm because the resolving power of X-ray diffraction topography is about 2 μm. It is expected that the observable minimum spacing of dislocation array h_m may be about 5 μm. Therefore, the maximum tilt angle of sub-grain boundary θ_m may be estimated by

$$\theta_m \simeq |\boldsymbol{b}|/h_m \simeq 5.6\times10^{-5} \text{ rad.} (\simeq 12''). \tag{1}$$

The MoKα_1 radiation operated at 45 kV, 0.7 mA was employed as X-ray source. The effective focal size was 50 μmϕ. For MoKα_1 radiation μt was $\sim$0.8 where μ is a linear absorption coefficient of LiF and t the specimen thickness. Exposure times of about 2 h/mm were enough with both Sakura nuclear plate E1 (emulsion thickness 50 μm) and Ilford nuclear plate L4 (emulsion thickness 50 μm). All topographs to be presented are negative, therefore, the black contrast indicates the enhanced diffraction intensity. And vertical direction of them is [001] and horizontal [010].

3. Geometry of Sub-grain boundaries

Geometrical features of sub-grain boundaries in NaCl structure predicted by the dislocation theory [1,10] will be mentioned briefly and we will discuss the possibility to observe them by X-ray diffraction topography in this section.

3.1. Sub-grain boundaries consisting of parallel dislocation array

The first one is a symmetrical pure tilt boundary consisting of edge dislocations having same Burgers vector parallel to the rotation axis existing in {110} boundary surface. Three typical planes, (101), (011), and (110) planes, are considered as the boundary surface. When edge dislocations exist on these planes, their Burgers vectors can be determined from $\boldsymbol{g}\cdot\boldsymbol{b}=0$ criterion. Since geometrical relation between the projection plane and the boundary surface give us information of observable images, these three type boundaries can be distinguished.

The second one is an asymmetrical pure tilt boundaries consisting of two types of edge dislocations with mutually perpendicular Burgers vectors, for example $a/2[110]$ and $a/2[1\bar{1}0]$. The planes included mutually perpendicular Burgers vectors are the cube ones. Therefore, the boundary surface is one of the $(h\ k\ 0)$, $(h\ 0\ l)$ and $(0\ k\ l)$ planes which are perpendicular to cube ones.

The third one is another asymmetrical pure tilt boundaries with Burgers vectors enclosing an angle of 60° (or 120°), for example $a/2[1\bar{1}0]$ and $a/2[10\bar{1}]$. In this case, a pair of two Burgers vectors exists on one of four {111} planes. Therefore, the boundary surface is the plane which is perpendicular to the {111} planes. In the particular example, the boundary surface $(h\ k\ l)$ is such that $h+k+l=0$. Many cases of this type can be considered and in many cases one of a pair of dislocations disappear due to $\boldsymbol{g}\cdot\boldsymbol{b}=0$. Many of observable tilt boundaries by the X-ray topography probably are of this type.

3.2. Sub-grain boundaries consisting of dislocation networks.

The model for a twist boundary having a [100] rotation axis and a (100) boundary plane consists of a square grid of pure screw dislocations having direction [011] and $[01\bar{1}]$ and Burgers vectors $a/2[011]$ and $a/2[01\bar{1}]$, respectively. If the contact plane deviates from the cube planes, the network acquires rhombus shaped meshes. The square grid of this type have been revealed in the alkali halides by decoration [6,7]. It was found that at the intersection points small segments of $a[100]$ dislocation develope sometimes according to the reaction

$$a/2[110]+a/2[1\bar{1}0]\rightarrow a[100]. \qquad (2)$$

When we observe this type sub-boundary by the X-ray diffraction topography, a square grid will be observed but no contrast appear at node points for $\boldsymbol{g}=[010]$ and no contrast will be observed for $\boldsymbol{g}=[001]$ and both a square grid and node points will be observed for $\boldsymbol{g}=[110]$.

If the contact plane of the boundary is the (111) plane, and if the rotation axis parallel to the [111] direction, the model for the boundary consists of an hexagonal grid of screw dislocations having Burgers vectors $a/2[1\bar{1}0]$, $a/2[\bar{1}01]$ and $a/2[01\bar{1}]$. Provided the rotation axis remains the same, a change in boundary plane only causes a change in the mesh shape, the pattern becomes such that its projection along [111] on (111) plane produces the same hexagonal net. As $\boldsymbol{g}\cdot\boldsymbol{b}=0$ criterion is satisfied for one of three dislocations constituting the network in many cases of topograpy, observation of complete hexagonal networks is difficult.

4. Experimental Results and Discussion

We performed X-ray topographic observations on about a thousand sub-grain boundaries. Though the probability of observing a dislocation array or a network is very small, we can observe them in some cases. Some topographs in which dislocations constituting sub-boundary are revealed are shown as follows.

Photo 1 (a) shows a topograph where Pendellösung fringes reported previously [8] are seen along the sub-grain boundary but no images of dislocations constituting sub-boundary are resolved. The direction of cutting line of sub-boundary with the (100) plane is the [001] direction. It is found from the measurement of spacing of Pendellösung fringe according to previous calculation[8] that this boundary plane makes an angle of about 45° to the (100) plane, that is, this plane is near the (110) plane. Dislocations constituting this boundary are the direction of [001] on the (110) plane and this sub-grain boundary is a symmetrical pure tilt one. An individual dislocation existing in sub-boundary was featureless not because the dislocation array did not exist, but because the dislocation array was too dense to form distinguishable images. Then, as the tilt angle between two adjusting sub-grain is comparatively large, X-ray diffraction at one side of the specimen can not undergo Bragg reflection so that the left side of the topograph is out of contrast. Such a sub-boundary where Pendellösung fringe appeared but no dislocation image are seen is often observed.

Photo 1 (b) shows a topograph of the sub-grain boundary consisting of dislocation array running nearly parallel to the [001] direction but slightly curved. From geometrical relationship among the observable range of this boundary, the specimen thickness and the projection direction it is found that the boundary surface exist on the (110). It seems that the structure of this sub-boundary is the same as that of photo 1 (a), and the dislocation array appeared but no Pendellösung fringes appeared because of its very small tilt angle. Determination of the Burgers vectors of the dislocations could not be made because the topographs taken by other diffraction planes are too faint.

Photo 2 (a) and (b) show topographs of sub-grain boundaries where dislocations lined with nearly equal interval along the $[0\bar{1}1]$ direction. These topographs show also that each dislocation forming the dislocation array is nearly perpendicular to the $[0\bar{1}1]$ direction, that is, its direction is [011], and its length is short (100 μm). Such dislocation images can be obtained when the dislocation lines which lie on the (011) plane and run along the [100] direction in the specimen are projected on the nuclear plate which is the inclined to the (100) plane by the angle of θ_B as described above. And they are determined to be edge dislocations by analysing their Burgers vectors. From these results it is concluded that they constitute symmetrical pure tilt boundary of which tilt angle is about 2×10^{-5} rad. (4″) estimated by eq (1).

Photo 3 (a) and (b) show topographs of sub-grain boundary where both Pendellösung fringes and the dislocation array are observed to overlap each other. The estimated tilt angle of this sub-boundary is about 3×10^{-6} rad. (1″) and the angle between this boundary surface and the (100) plane is estimated to be smaller than 10° by measuring the spacing of Pendellösung fringes. Then, the relatively long images of dislocation constituting sub-boundary are seen. Though their Burgers vectors were not determined because of inferior topographs taken by other diffraction planes, from the geometry of this sub-boundary, this boundary seems to be an asymmetrical pure tilt boundary.

Photo 4 (a) and (b) show topographs of sub-grain boundaries where square grid dislocation networks are seen. In this case, we used two specimens which were cleaved from one specimen so that their surfaces were matched each other. Then, the sub-boundary shown in photo 4 (a) continues on one in photo 4 (b). Their Burgers vectors were determined by taking topographs with $\boldsymbol{g}=[0\bar{1}1]$ and $\boldsymbol{g}=[011]$. This result indicated that they were screw dislocations. This contact plane lies nearly on the (100) plane. Then, this sub-boundary proved to be twist boundary. Photo 5 shows a stereo pair of topographs of this boundary where (a) taken with $\boldsymbol{g}=[010]$ and (b) $\boldsymbol{g}=[0\bar{1}0]$. If a stereoscope is used to observe this pair, its structure is seen three-dimensionally but it is exaggerated by the high magnification of topographs. Photo 6 (a) shows the enlarged topograph of photo 4 (b) and photo 6 (b) shows the same region but taken with $\boldsymbol{g}=[011]$. In photo 6 (a) the images of the nodes crossing a square grid network disappeared but in photo 6 (b) intense contrast is observed the position corresponding to nodes. This result indicated that Burgers vector of dislocations at nodes have $a[001]$ as predicted by eq (2).

Photo 7 shows a topograph of sub-boundary where an hexagonal dislocation network constituting twist boundary is seen. This topograph is very interesting though further analysis were not made because of geometrical difficulties.

Some observations concerning to changes of sub-grain boundaries in crystal under annealing have been reported previously by the author [9]. More detailed observation and analysis are made here. Photo 8 (a), (b) and (c) show topographs taken with various diffraction vectors where parallel lined dislocations along a grain boundary are seen. In general, the configuration of dislocations tend to lie in linear form during an annealing process because dislocations can climb and react among them [9]. It seems that these dislocation lines observed here are rearranged by annealing. Analysis of these dislocations showed that they were edge dislocations and existed on (110) plane. This result indicate that geometrical feature of them is in good agreement with the symmetrical small tilt boundary as shown in photo 2. If the dislocation array constitutes such a tilt boundary, its tilt angle must be very small according to eq (1). However, photo 8 show that images of an adjusting grain did not appear clearly and the reflection with strong intensity were seen along grain boundary. Then, its tilt angle was considered to be large compared with estimated one so that this is different from small tilt sub-boundary. This boundary may be considered as a coincidence site grain boundary of which models have been proposed by many workers [11~14].

5. Conclusion

Sub-grain boundaries in LiF single crystal were observed by limited projection topography and analysis was made on some sub-grain boundaries where dislocations constituting them are resolved. The results of observa-

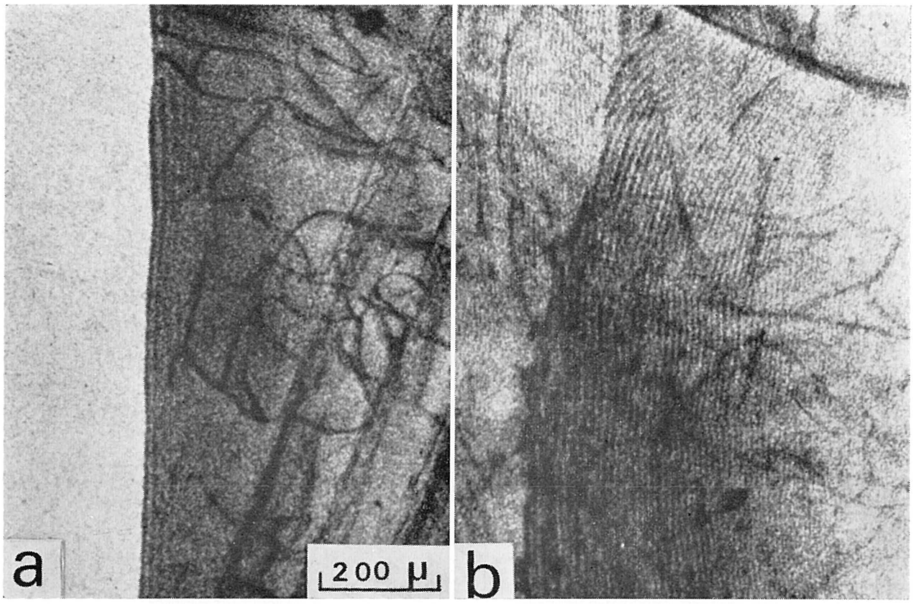

Photo 1. The topographs of symmetrical pure tilt boundaries taken with $\boldsymbol{g}=$ [010] (a) Pendellösung fringes are seen. (b) Parallel dislocation arraies nearly along a [001] are seen. For all topographs presented vertical direction of them is [001] and horizontal [010].

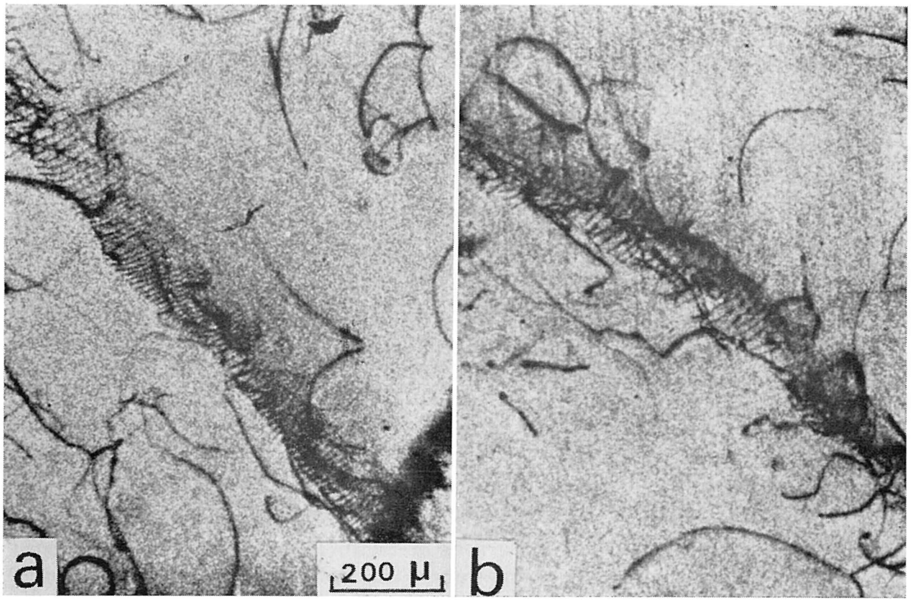

Photo 2. The topographs of symmetrical pure tilt boundaries taken with $\boldsymbol{g}=$ [010]. Boundary surface exists on (011).

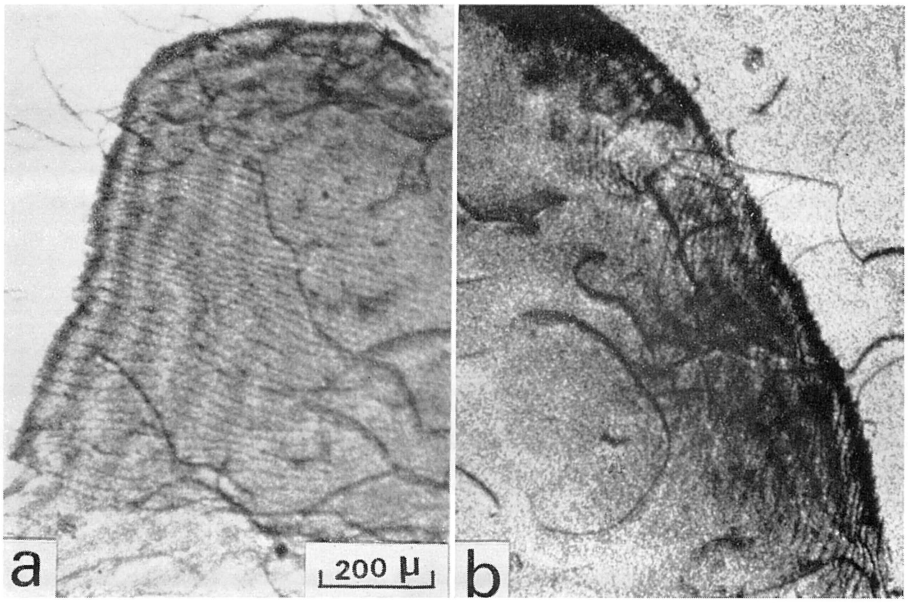

Photo 3. The topographs of asymmetrical pure tilt boundaries taken with $\boldsymbol{g}=[010]$. Pendellösung fringe and dislocation array are seen to overlap each other.

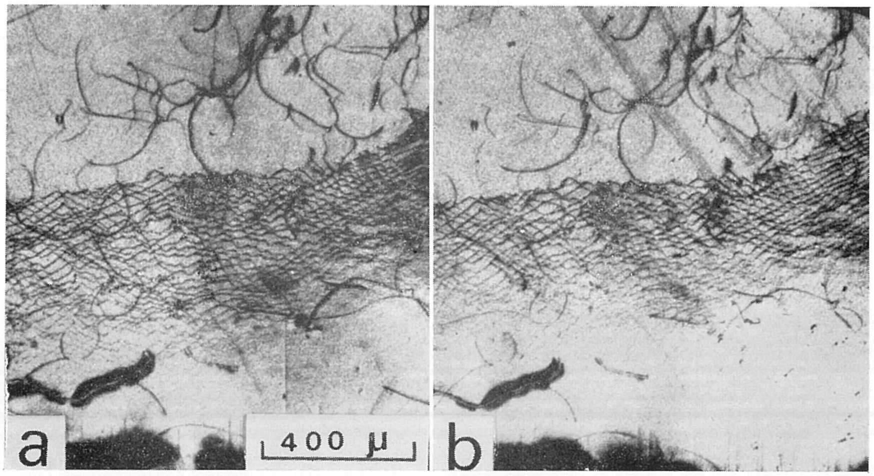

Photo 5. A stereo pair of topographs of Photo 4 (b). If a stereoscope is used to observe, three-dimensional structure are seen. (a) was taken with $\boldsymbol{g}=[010]$, (b) with $\boldsymbol{g}=[0\bar{1}0]$.

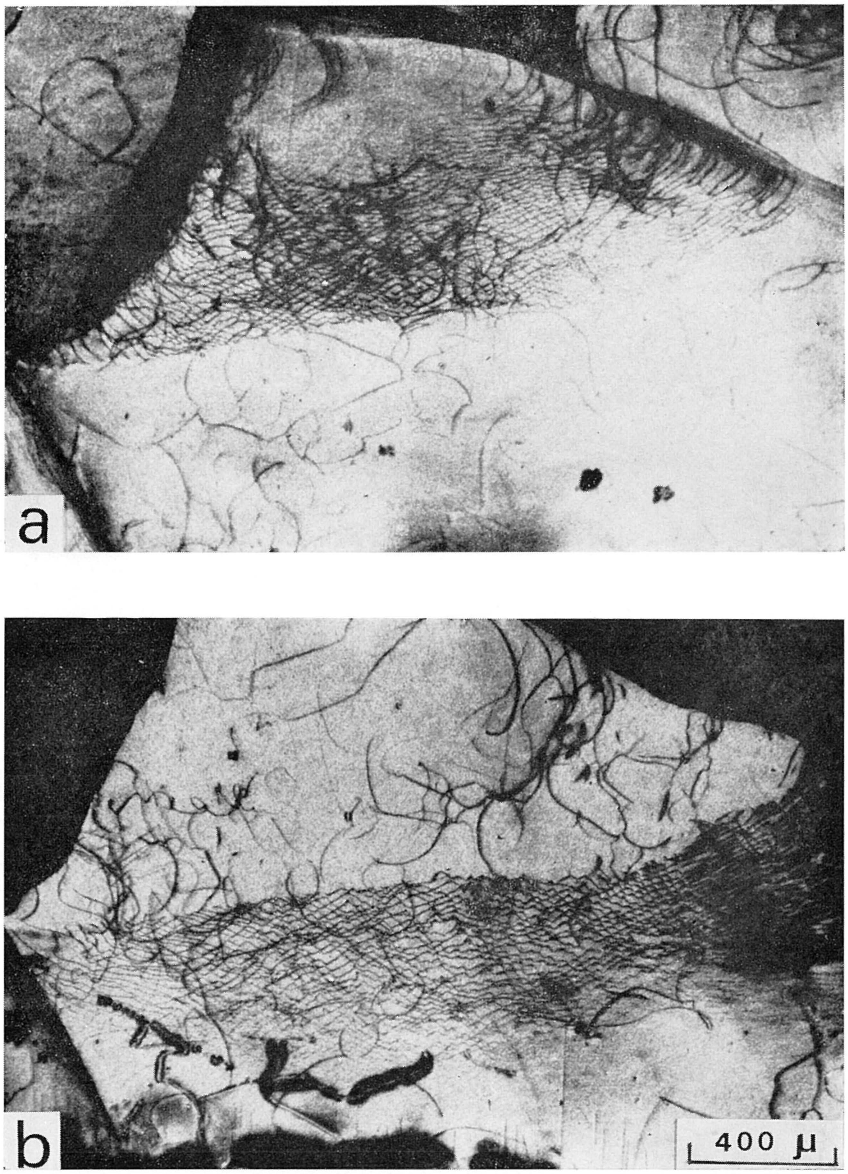

Photo 4. The topographs of twist boundaries taken with $\boldsymbol{g}=[010]$. Square grid dislocation networks are seen. The network on (a) continues to that on (b).

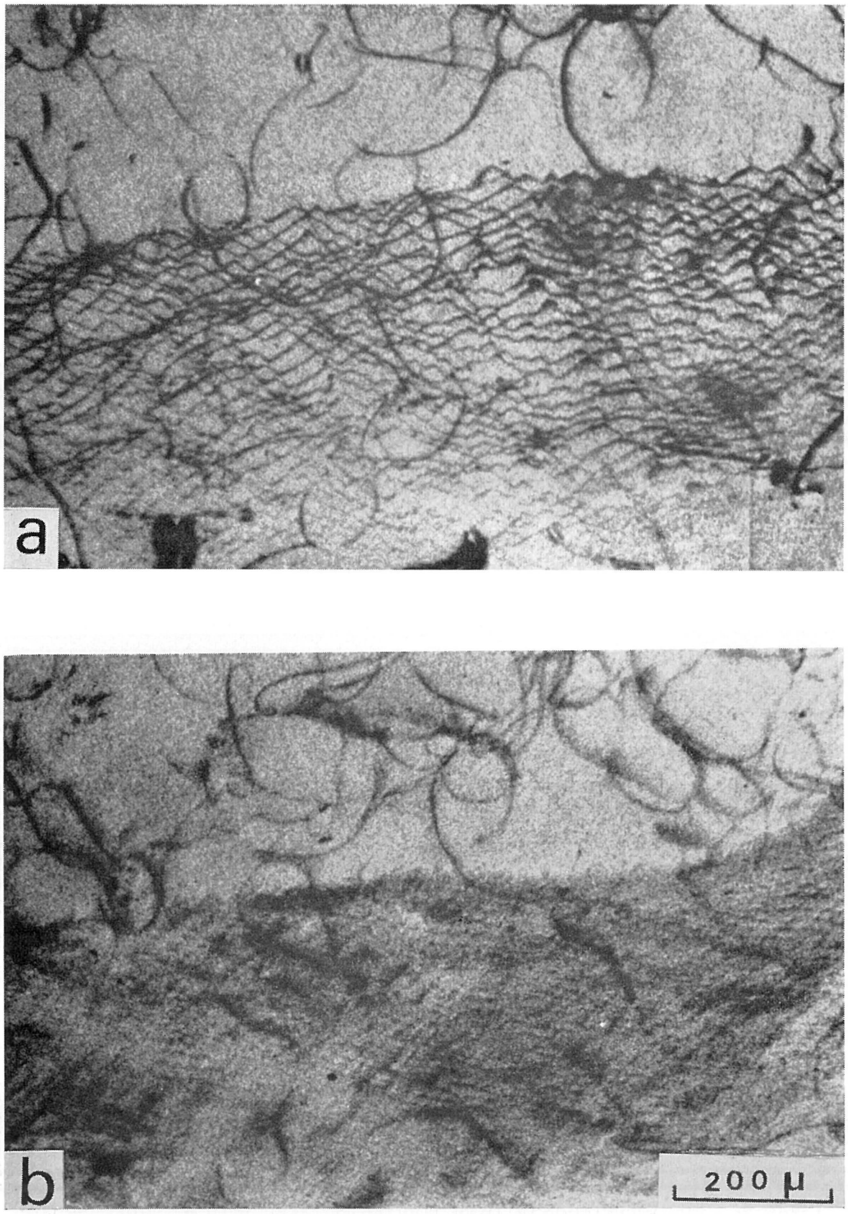

Photo 6. The enlargement of a part of Photo 4 (b). (a) was taken with $\boldsymbol{g}=[010]$, (b) with $\boldsymbol{g}=[011]$.

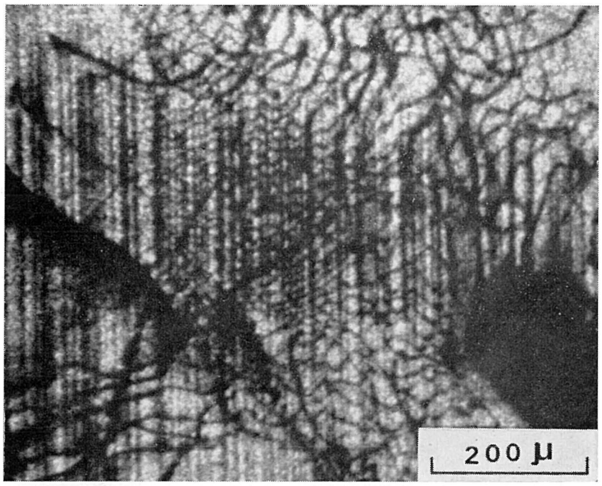

Photo 7. The topograph of a hexagonal grid dislocation networks taken with $\boldsymbol{g}=[010]$.

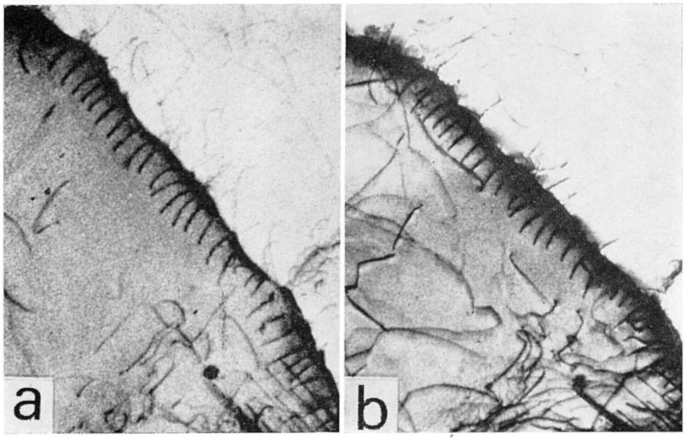

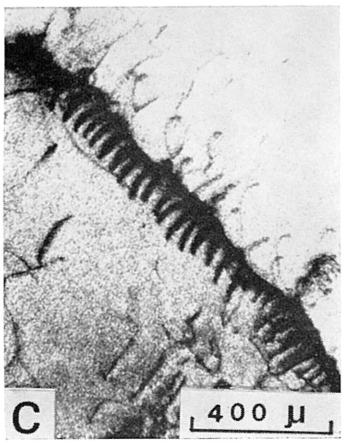

Photo 8. The topographs of grain boundaries in annealed specimen. Parallel lined dislocation along a grain boundary are seen. (a) was taken with $\boldsymbol{g}=[010]$, (b) with $\boldsymbol{g}=[001]$, (c) with $\boldsymbol{g}=[0\bar{1}1]$.

tion made possible the direct verification of models predicted by the dislocation theory.

This experiment showed also the superiority of limited projection topography for the direct observation of dislocations with good resolution.

Acknowledgments

The author wishes to thank Mr. Y. Akashi for several helpful discussion and Mr. K. Araki for his aids in experimental works. This work was partially supported by the Grand-in-Aid for Fundamental Scientific Research.

References

1) Amelinckx, S., *The Direct Observation of Dislocations,* Academic press, New York, London, 1964.
2) Vogel, F.L., Pfann, W.G., Correy, H.E. and Thomas, E.E., Observations of Dislocations in Lineage Boundaries in Germanium, Phys. Rev., Vol. 90, No, 3, 1953, p. 489.
3) Vogel, F.L.Jr., Dislocations in Low-Angle Boundaries in Germanium, Acta Met., Vol. 3, 1955, p. 245.
4) Okuda, J., Observations of Dislocations along Grain Boundaries in Germanium Crystals, J. Phy. Soc. Japan, Vol. 10, No. 11, 1955, p. 1018.
5) Mitohell, J.W. and Mott, N.F., The Nature and Formation of the Photographic Latent Image, Phil, Mag., Vol. 8, No. 2, 1957, p. 1149.
6) Amelinckx, S., Dislocations in Caesium Bromide, Phil. Mag. Vol. 8, No. 3, 1958, p. 307.
7) Amelinckx, S., Dislocation Patterns in Potassium Chloride, Acta, Met., Vol. 6, No. 1, 1958, p. 34.
8) Futagami, K., X-Ray Studies on the Sub-Grain Boundaries of LiF Single Crystals by the Limited Projection Topography, Japan J. appl. Phys., Vol. 6, No. 12, 1967, p. 1381.
9) Futagami, K., Study on Crystal Lattice Defect by the X-ray Diffraction Topography, Rep. Res. Inst. Appl. Mech., Vol. XVII, No. 57, 1969, p. 49.
10) Read, W.T. , *Dislocations in Crystals,* McGraw-Hill, New York, 1953.
11) Bollmann, W., *Crystal Defects and Crystalline Interfaces,* Springer-Verlag Berlin. Heidelberg. New York, 1970.
12) Ishida, Y. and Brown, M.H., Dislocations in Grain Boundaries and Grain Boundary Sliding, Acta Met., Vol. 15, No. 5, 1967, p. 857.
13) Ishida, Y., Hasegawa, T. and Nagata, F., Grain Boundary Fine Structure in an Iron Alloy, J. appl. Phys., Vol. 40, No. 5, 1969, p. 2182.
14) Marcinkowski, M.J., Tseng, W.F. and Dwarakadasa, E.S., Relationship between Grain Boundary Dislocations, Moiré Patterns, and Diffraction Effects, Phys. stat. sol. (a), Vol. 22, No. 2, 1974, p. 659.

(Received November 30, 1974)